Appendix D. Time Discretizations

In this appendix we will make some general comments about time discretizations, survey standard methods for ODEs and their stability regions, discuss integrating factors for Fourier spatial discretizations, and highlight some low-storage time-discretization formulas that have been widely used in conjunction with spectral methods.

D.1 Notation and Stability Definitions

The typical evolution equation can be written

$$\begin{aligned} &\frac{\partial u}{\partial t} = f(u,t) \ , \quad t > 0, \\ &u(0) = 0 \ , \end{aligned} \tag{D.1.1}$$

where the (generally) nonlinear operator f contains the spatial part of the PDE. Following the general formulation of Chap. 6, the semi-discrete version is

$$Q_N \frac{\mathrm{d}u^N}{\mathrm{d}t} = Q_N f_N(u^N, t) \ ,$$

where u^N is the spectral approximation to u, f_N denotes the spectral approximation to the operator f, and Q_N is the spatial projection operator which characterizes the scheme. Let us denote by $\mathbf{u}(t)$ the vector of the spatial unknowns which determine $u^N(t)$. For example, in a collocation method for a Dirichlet boundary-value problem, $\mathbf{u}(t)$ represents the set of the interior grid-point values of $u^N(t)$. Then the previous discrete problem can be written in the form

$$\begin{aligned} &\frac{\mathrm{d}\mathbf{u}}{\mathrm{d}t} = \mathbf{f}(\mathbf{u},t) \ , \qquad t > 0, \\ &\mathbf{u}(0) = \mathbf{u}_0 \ , \end{aligned} \tag{D.1.2}$$

where $\mathbf{f}$ is the vector-valued function governing the semi-discrete problem. For Galerkin and G-NI methods, $\mathbf{f}$ may incorporate the matrix M^{-1}, where M

denotes the mass matrix which expresses the projection $Q_N \dfrac{\mathrm{d}u^N}{\mathrm{d}t}$ algebraically as $M\dfrac{\mathrm{d}\mathbf{u}}{\mathrm{d}t}$. For time-dependent, linear PDEs, (D.1.2) reduces to

$$\begin{aligned} &\frac{\mathrm{d}\mathbf{u}}{\mathrm{d}t} = -L\mathbf{u} + \mathbf{b} \ , \qquad t > 0, \\ &\mathbf{u}(0) = \mathbf{u}_0 \ , \end{aligned} \tag{D.1.3}$$

where L is the matrix representing the spatial discretization by the chosen spectral method. (The use of the negative sign in front of L in (D.1.3) is consistent with the notation of Chap. 4 – see (4.8) – for describing the discretization of a time-independent boundary-value problem. In that chapter, we introduced and analyzed some representative spectral discretization matrices.) This is also called a method-of-lines approach or a continuous-in-time discretization. In describing the time discretizations, we denote the time-step by Δt, the n-th time-level by $t_n = n\Delta t$, the approximate solution at time-step n by $\mathbf{u}^n$, and use $\mathbf{f}^n = \mathbf{f}(\mathbf{u}^n, t^n)$.

The corresponding (linear, scalar) model problem is

$$\frac{\mathrm{d}u}{\mathrm{d}t} = \lambda u \ , \tag{D.1.4}$$

where λ is a complex number, which for (D.1.2) is "representative" of the partial derivative of f with respect to u (in the scalar case) or of the eigenvalues of the Jacobian matrix $(\partial f_i/\partial u_j)_{i,j}$ in the vector case, and which for (D.1.3) is representative of the eigenvalues of $-L$.

In most applications of spectral methods to partial differential equations the spatial discretization is spectral but the temporal discretization uses conventional finite differences. (See, however, Morchoisne (1979, 1981) and Tal-Ezer (1986a, 1989) for some exploratory work on methods using spectral discretizations in both space and time. See also Schötzau and Schwab (2000) for high-order discontinuous Galerkin methods in time, albeit coupled with the *hp*-version of finite elements rather than with spectral methods.) Some standard references from the extensive literature on numerical methods for ODEs are the books by Gear (1971), Lambert (1991), Shampine (1994), Hairer, Norsett and Wanner (1993), Hairer and Wanner (1996), and Butcher (2003).

If the spatial discretization is presumed fixed, then we use the term stability in its ODE context. The time discretization is said to be *stable* (sometimes called *zero-stable*) if there exist positive constants δ, ε and $C(T)$, independent of Δt, such that, for all $T > 0$ (perhaps limited by a maximal T_{max} depending on the problem) and for all $0 \le \Delta t < \delta$,

$$\|\mathbf{u}^n - \mathbf{v}^n\| \le C(T)\|\mathbf{u}^0 - \mathbf{v}^0\| \qquad \text{for } 0 \le t_n \le T \tag{D.1.5}$$

provided that $\|\mathbf{u}^0 - \mathbf{v}^0\| < \varepsilon$, where $\|\mathbf{u}^n\|$ is some spatial norm of $\mathbf{u}^n$. The constant $C(T)$ is permitted to grow with T. Here, $\mathbf{v}^n$ is the solution obtained

by the same numerical method corresponding to a (perturbed) initial data $\mathbf{v}^0$. On a linear problem (hence in particular, for the problems (D.1.3) or (D.1.4)), (D.1.5) can be equivalently replaced by

$$\|\mathbf{u}^n\| \leq C(T)\|\mathbf{u}^0\| \qquad \text{for } 0 \leq t_n \leq T\,. \tag{D.1.6}$$

For many problems involving integration over long time intervals, a method which admits the temporal growth allowed by the estimate (D.1.5) is undesirable. As one example, take a problem of the form (D.1.2) for which $(\partial f/\partial u)(w,t)$ is negative for all w and t, or more generally, for which f satisfies the *right Lipschitz condition*: there exists $\mu < 0$ such that

$$\langle f(u,t) - f(v,t), u - v\rangle \leq \mu\|u - v\|^2 \qquad \text{for all } u, v, t,$$

where $\langle\cdot,\cdot\rangle$ is a suitable scalar product and $\|\cdot\|$ its associated norm. In these cases,

$$\|u(t) - v(t)\| \leq e^{\mu t}\|u(0) - v(0)\|\,.$$

(Such problems are referred to as dissipative Cauchy problems in the ODE literature.) The ODEs resulting from spectral spatial discretizations of the heat equation (with homogeneous boundary data and zero source term) fall into this category. In this case one desires that the time discretization be *asymptotically stable*, i.e., that instead of (D.1.5) it satisfy the stronger requirement

$$\|\mathbf{u}^n - \mathbf{v}^n\| \to 0 \quad \text{as} \quad t_n \to +\infty, \tag{D.1.7}$$

or that it be *contractive* (or *B-stable*):

$$\|\mathbf{u}^n - \mathbf{v}^n\| \leq C\|\mathbf{u}^{n-1} - \mathbf{v}^{n-1}\| \qquad \text{for all } n \geq 1, \tag{D.1.8}$$

for a suitable constant $C < 1$ independent of n.

As another example for which the above notion of stability is too weak, consider ODEs resulting from the spatial discretization of linear, spatially periodic, purely hyperbolic systems. For these problems, asymptotic stability for the time discretization is undesirable since the exact solution is undamped in time. Instead we rather desire a time discretization which is *temporally stable*, for which we merely require that

$$\|\mathbf{u}^n\| \leq \|\mathbf{u}^0\| \qquad \text{for all } n \geq 1\,. \tag{D.1.9}$$

The notion of *weak instability* is sometimes used in a loose sense for schemes which admit solutions to periodic hyperbolic problems which grow with time, but for which the growth rate decreases with Δt. For example, the constant $C(T)$ in (D.1.5) might have the form

$$C(T) = e^{\alpha(\Delta t)^p T}\,,$$

where $\alpha > 0$ and p is a positive integer. For such weakly unstable schemes, the longer the time interval of interest, i.e., the larger is T, the smaller must

Δt be chosen to keep the spurious growth of the solution within acceptable bounds.

Another notion that is relevant to periodic, hyperbolic problems is that of *reversible* (or *symmetric*) time discretizations. These are schemes for which the solution may be marched forward from t^n to t^{n+1} and then backwards to t^n with the starting solution at t^n recovered exactly (except for round-off errors).

Two final definitions are in order for our subsequent discussion. The *absolute stability region* (often referred to just as the *stability region*), say $\mathcal{A}$, of a numerical method is customarily defined for the scalar model problem (D.1.4) to be the set of all complex numbers $\alpha = \lambda \Delta t$ such that any sequence $\{u^n\}$ generated by the method with such λ and Δt satisfies $\|u^n\| \leq C$ as $t_n \to \infty$, for a suitable constant C. Furthermore, a method is called *A-stable* if the region of absolute stability includes the region $\mathrm{Re}(\lambda \Delta t) < 0$. We warn the reader that in some books the absolute stability region is defined as the set of all $\lambda \Delta t$ such that $\|u^n\| \to 0$ as $t_n \to \infty$. This new region, say $\mathcal{A}^0$, would not necessarily coincide with $\mathcal{A}$. In general, if $\mathcal{A}^0$ is non-empty, $\mathcal{A}$ is its closure. However, there are cases for which $\mathcal{A}^0$ is empty (e.g., the midpoint or leap-frog method) and $\mathcal{A}$ is not ($\mathcal{A} = \{z = \alpha i,\ -1 \leq \alpha \leq 1\}$ for the midpoint method). Finally, we note that zero-stable methods are those for which $\mathcal{A}$ contains the origin $z = 0$ of the complex plane.

As noted by Reddy and Trefethen (1990, 1992), having the eigenvalue scaled by the time-step Δt falling within the absolute stability region of the ODE method is not always sufficient for stability of the computation. They present a stability criterion utilizing ϵ-pseudospectra. As noted in Sect. 4.3.2, first-derivative (indeed, any odd-order derivative) matrices for nonperiodic problems are nonnormal. However, as discussed by Trefethen (2000, Chapter 10), in almost all cases the "rule-of-thumb" condition involving the standard eigenvalues is acceptable.

On the other hand, we may be interested in the behavior of the computed solution as both the spatial and temporal discretizations are refined. We now define stability by an estimate of the form (D.1.5) where C is independent of Δt, ε and the spatial discretization parameter N, the norm is independent of N, but δ will in general be a function of N. The functional dependence of δ upon N which is necessary to obtain an estimate of the form (D.1.5) is termed the *stability limit* of the numerical method. If δ is in fact independent of N, then the method is called *unconditionally stable*. Clearly, a necessary condition for the fully discrete problem to be stable is that the semi-discrete problem be stable in the sense discussed in Sect. 6.5. Likewise, a *temporal* stability limit for the fully discrete scheme for a hyperbolic system is the functional dependence of δ upon N which is necessary to obtain an estimate of the form (D.1.9).

D.2 Standard ODE Methods

In this section we furnish as a convenience the basic formulas and diagrams for the absolute stability regions for those time discretizations of (D.1.2) that are most commonly used in conjunction with spectral discretizations in space. Among the factors which influence the choice of a time discretization are the accuracy, stability, storage requirements, and work demands of the methods. The storage and work requirements of a method can be deduced in a straight-forward manner from the definition of the method and the nature of the PDE. The accuracy of a method follows from a truncation error analysis and the stability for a given problem is intimately connected with the spectrum of the spatial discretization. In this section we will describe some of the standard methods for ODEs and relate their stability regions to the spectra of the advection and diffusion operators. Bear in mind that in many problems different time discretizations are used for different spatial terms in the equation. The illustrations of the spectra of the spectral differentiation, mass and stiffness matrices furnished in Sect. 4.3 combined with the stability diagrams in this section suffice for general conclusions to be drawn on appropriate choices of time-discretization methods and time-step limits for temporal stability.

For the reader's convenience, Table D.1 provides the numerical values of the intersections of the absolute stability regions with the negative real axis and the positive imaginary axis for all methods discussed in this section.

D.2.1 Leap Frog Method

The *leap frog* (LF) *method* (also called the *midpoint method*) is a second-order, two-step scheme given by

$$\mathbf{u}^{n+1} = \mathbf{u}^{n-1} + 2\Delta t \mathbf{f}^n \ . \tag{D.2.1}$$

This produces solutions of constant norm for the model problem provided that $\lambda\Delta t$ is on the imaginary axis and that $|\lambda\Delta t| \leq 1$ (see Table D.1). Thus, leap frog is a suitable explicit scheme for problems with purely imaginary eigenvalues. It also is a reversible, or symmetric, method. However, since it is only well-behaved on a segment in the complex $\lambda\Delta t$-plane for the model problem, extra care is needed in practical situations.

The most obvious application is to periodic advection problems, for the eigenvalues of the Fourier approximation to $\mathrm{d}/\mathrm{d}x$ are imaginary. The difficulty with the leap frog method is that the solution is subject to a temporal oscillation with period $2\Delta t$. This arises from the extraneous (spurious) solution to the temporal difference equations. The oscillations can be controlled by every so often averaging the solution at two consecutive time-levels.

Leap frog is quite inappropriate for problems whose spatial eigenvalues have nonzero real parts. This certainly includes diffusion operators. Leap frog

is also not viable for advection operators with nonperiodic boundary conditions. The figures in Sect. 4.3.2 indicate clearly that the discrete spectra of Chebyshev and Legendre approximations to the standard advection operator have appreciable real parts.

D.2.2 Adams-Bashforth Methods

This is a class of explicit multistep methods which includes the simple *forward Euler* (FE) *method*

$$\mathbf{u}^{n+1} = \mathbf{u}^n + \Delta t \mathbf{f}^n \ , \tag{D.2.2}$$

the popular *second-order Adams-Bashforth* (AB2) *method*

$$\mathbf{u}^{n+1} = \mathbf{u}^n + \tfrac{1}{2}\Delta t \left[3\mathbf{f}^n - \mathbf{f}^{n-1}\right] \ , \tag{D.2.3}$$

the still more accurate *third-order Adams-Bashforth* (AB3) *method*

$$\mathbf{u}^{n+1} = \mathbf{u}^n + \tfrac{1}{12}\Delta t \left[23\mathbf{f}^n - 16\mathbf{f}^{n-1} + 5\mathbf{f}^{n-2}\right] \ , \tag{D.2.4}$$

and the *fourth-order Adams-Bashforth* (AB4) *method*

$$\mathbf{u}^{n+1} = \mathbf{u}^n + \tfrac{1}{24}\Delta t \left[55\mathbf{f}^n - 59\mathbf{f}^{n-1} + 37\mathbf{f}^{n-2} - 9\mathbf{f}^{n-3}\right] \ . \tag{D.2.5}$$

These methods are not reversible.

The stability regions $\mathcal{A}$ of these methods are shown in Fig. D.1 (left) and the stability boundaries along the axes are given in Table D.1. Note that the size of the stability region decreases as the order of the method increases. Note also that except for the origin, no portion of the imaginary axis is included in the stability regions of the first- and second-order methods, whereas the third- and fourth-order versions do have some portion of the imaginary axis included in their stability regions. Nevertheless, the AB2 method is weakly unstable, i.e., for a periodic, hyperbolic problem the acceptable Δt decreases at T increases.

As is evident from Fig. D.1 (left), higher order AB methods are temporally stable for Fourier approximations to periodic advection problems. Let the upper limit of the absolute stability region along the imaginary axis be denoted by c. Then the temporal stability limit is

$$\frac{N}{2}\Delta t \leq c$$

or

$$\Delta t \leq \frac{c}{\pi}\,\Delta x \ . \tag{D.2.6}$$

The limit on Δt is smaller by a factor of π than the corresponding limit for a second-order finite-difference approximation in space. The Fourier spectral approximation is more accurate in space because it represents the high-frequency components much more accurately than the finite-difference

method. The artificial damping of the high-frequency components which is produced by finite-difference methods enables the stability restriction on the time-step to be relaxed.

Chebyshev and Legendre approximations to advection problems appear to be temporally stable under all Adams-Bashforth methods for sufficiently small Δt; precisely, for $\Delta t \leq CN^{-2}$ for a suitable constant C. As discussed in Sect. 4.3.2, the spatial eigenvalues all have negative real parts. Thus, the failure of the AB2 method to include the imaginary axis in its absolute stability region does not preclude temporal stability.

The temporal stability limits for Adams-Bashforth methods for Fourier, Chebyshev and Legendre approximations to diffusion equations are easy to deduce since their spatial eigenvalues (i.e., the eigenvalues of the matrix $-L$, where $L = B^{-1}A$ is the matrix considered in Sect. 4.3.1) are real and negative (limited in modulus as indicated in Table 4.2), and the stability bounds along the negative real axis are provided in Table D.1. In this case, Δt should be limited by a constant times N^{-2} for Fourier approximations, by a constant times N^{-4} for Chebyshev or Legendre collocation approximations, by a constant times N^{-3} for Legendre G-NI approximations. This follows from the eigenvalue analysis that is carried out in Chap. 4.

D.2.3 Adams-Moulton Methods

A related set of implicit multistep methods are the Adams-Moulton methods. They include the *backward Euler* (BE) *method*

$$\mathbf{u}^{n+1} = \mathbf{u}^n + \Delta t \mathbf{f}^{n+1} , \tag{D.2.7}$$

the *Crank-Nicolson* (CN) *method*

$$\mathbf{u}^{n+1} = \mathbf{u}^n + \tfrac{1}{2}\Delta t[\mathbf{f}^{n+1} + \mathbf{f}^n] , \tag{D.2.8}$$

the *third-order Adams-Moulton* (AM3) *method*

$$\mathbf{u}^{n+1} = \mathbf{u}^n + \tfrac{1}{12}\Delta t[5\mathbf{f}^{n+1} + 8\mathbf{f}^n - \mathbf{f}^{n-1}] , \tag{D.2.9}$$

and the *fourth-order Adams-Moulton* (AM4) *method*

$$\mathbf{u}^{n+1} = \mathbf{u}^n + \tfrac{1}{24}\Delta t[9\mathbf{f}^{n+1} + 19\mathbf{f}^n - 5\mathbf{f}^{n-1} + \mathbf{f}^{n-2}] . \tag{D.2.10}$$

Forward Euler (FE) (see D.2.2), backward Euler (BE) and Crank-Nicolson (CN) methods are special cases of *θ-methods*, defined as

$$\mathbf{u}^{n+1} = \mathbf{u}^n + \Delta t[\theta\mathbf{f}^{n+1} + (1-\theta)\mathbf{f}^n] , \tag{D.2.11}$$

for $0 \leq \theta \leq 1$. Precisely, they correspond to the choice $\theta = 0$ (FE), $\theta = 1$ (BE) and $\theta = 1/2$ (CN). All θ-methods except for FE are implicit. All θ-methods are first-order accurate, except for CN, which is second-order. For each $\theta < \frac{1}{2}$,

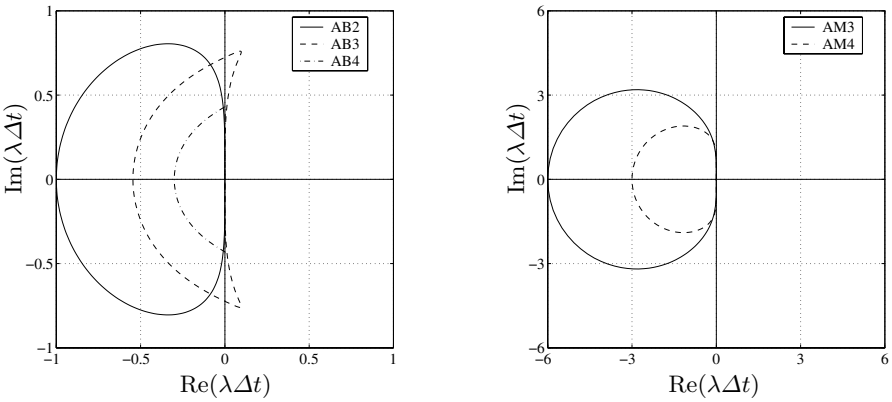

Fig. D.1. Absolute stability regions of Adams-Bashforth (*left*) and Adams-Moulton (*right*) methods

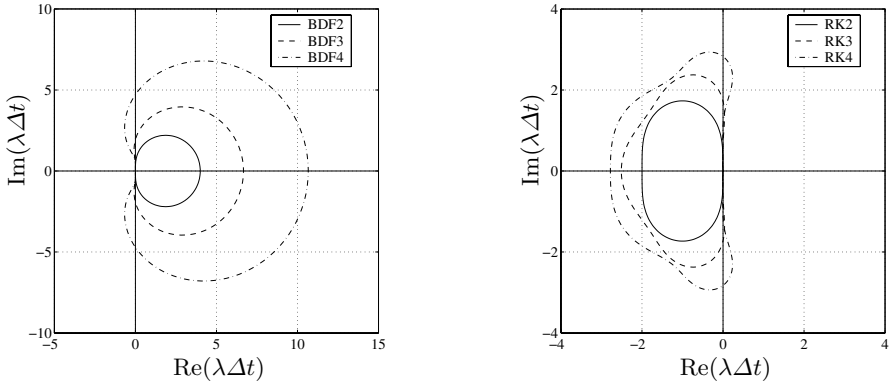

Fig. D.2. Absolute stability regions of backwards-difference formulas (*left*) and Runge-Kutta methods (*right*). The BDF methods are absolutely stable on the exteriors (and boundaries) of the regions enclosed by the curves, whereas the RK methods are absolutely stable on the interiors (and boundaries) of the regions enclosed by the curves

the absolute stability region is the circle in the left half-plane $\mathrm{Re}(\lambda\Delta t) \leq 0$ with center $z = (2\theta - 1)^{-1}$ and radius $r = (1 - 2\theta)^{-1}$. The stability region of the CN method coincides with the half-plane $\mathrm{Re}(\lambda\Delta t) \leq 0$. For each $\theta > \frac{1}{2}$, the absolute stability region is the exterior of the open circle in the right half-plane $\mathrm{Re}(\lambda\,\Delta t) > 0$ with center $z = (2\theta - 1)^{-1}$ and radius $r = (2\theta - 1)^{-1}$. Thus, all θ-methods for $\frac{1}{2} \leq \theta \leq 1$ are A-stable.

The absolute stability regions of the third- and fourth-order Adams-Moulton methods are displayed in Fig. D.1 (right) and the stability boundaries along the axes are given in Table D.1. In comparison with the explicit

Table D.1. Intersections of absolute stability regions with the negative real axis (left) and with the positive imaginary axis (right)

Method	$\mathcal{A} \cap \mathbb{R}_-$	$\mathcal{A} \cap i\mathbb{R}_+$
Leap frog (midpoint)	$\{0\}$	$[0, 1]$
Forward Euler	$[-2, 0]$	$\{0\}$
Crank-Nicolson	$(-\infty, 0]$	$[0, +\infty)$
Backward Euler	$(-\infty, 0]$	$[0, +\infty)$
θ-method, $\theta < 1/2$	$[2/(2\theta - 1), 0]$	$\{0\}$
θ-method, $\theta \geq 1/2$	$(-\infty, 0]$	$[0, +\infty)$
AB2	$(-1, 0]$	$\{0\}$
AB3	$[-6/11, 0]$	$[0, 0.723]$
AB4	$[-3/10, 0]$	$[0, 0.43]$
AM3	$[-6, 0]$	$\{0\}$
AM4	$[-3, 0]$	$\{0\}$
BDF2	$(-\infty, 0]$	$[0, +\infty)$
BDF3	$(-\infty, 0]$	$[0, 1.94)$
BDF4	$(-\infty, 0]$	$[0, 4.71)$
RK2	$[-2, 0]$	$\{0\}$
RK3	$[-2.51, 0]$	$[0, 1.73]$
RK4	$[-2.79, 0]$	$[0, 2.83]$

Adams-Bashforth method of the same order, an Adams-Moulton method has a smaller truncation error (by factors of five and nine for second and third-order versions), a larger stability region, and requires one fewer levels of storage. However, it does require the solution of an implicit set of equations. The CN method is reversible; the others are not.

The CN method is commonly used for diffusion problems. In Navier-Stokes calculations, it is frequently applied to the viscous and pressure gradient components. Although CN is absolutely stable for the former and temporally stable for the latter, it has the disadvantage that it damps high-frequency components very weakly, whereas in reality these components decay very rapidly. Deville, Kleiser and Montigny-Rannou (1984) have noted that this is undesirable in Navier-Stokes applications for which the solution itself decays rapidly. One remedy is to resort to BE – it damps the high frequency components rapidly. An alternative approach is to use the θ-method (D.2.11) for $\theta = 1/2 + \alpha\Delta t$, where α is a small positive constant. This method damps all components of the solution, and although it is formally first-order accurate in time (if $\alpha > 0$) it is "effectively" second order if $\alpha \ll 1$.

The Adams-Moulton methods of third and higher order are only conditionally stable for advection and diffusion problems. The stability limits

implied by Fig. D.1 indicate that the stability limit of a high-order Adams-Moulton method is roughly ten times as large for a diffusion problem as the stability limit of the corresponding Adams-Bashforth method. In addition, AM3 and AM4 are weakly unstable for Fourier approximations to advection problems, since the origin is the only part of the imaginary axis which is included in their absolute stability regions.

D.2.4 Backwards-Difference Formulas

Another class of implicit time discretizations is based upon backwards-difference formulas . These include the *first-order backwards-difference scheme* (BDF1), which is identical to backward Euler, the *second-order backwards-difference scheme* (BDF2)

$$\mathbf{u}^{n+1} = \tfrac{1}{3}[4\mathbf{u}^n - \mathbf{u}^{n-1}] + \tfrac{2}{3}\Delta t\mathbf{f}^{n+1} , \tag{D.2.12}$$

the *third-order backwards-difference scheme* (BDF3)

$$\mathbf{u}^{n+1} = \tfrac{1}{11}[18\mathbf{u}^n - 9\mathbf{u}^{n-1} + 2\mathbf{u}^{n-2}] + \tfrac{6}{11}\Delta t\mathbf{f}^{n+1} , \tag{D.2.13}$$

and the *fourth-order backwards-difference scheme* (BDF4)

$$\mathbf{u}^{n+1} = \tfrac{1}{25}[48\mathbf{u}^n - 36\mathbf{u}^{n-1} + 16\mathbf{u}^{n-2} - 3\mathbf{u}^{n-3}] + \tfrac{12}{25}\Delta t\mathbf{f}^{n+1} . \tag{D.2.14}$$

The absolute stability regions of these methods are displayed in Fig. D.2 (left) and the stability boundaries along the axes are given in Table D.1. The stability regions are much larger than those of the corresponding AM methods, but for orders higher than 2, BDF methods are unstable in a (small) region to the left of the imaginary axis.

D.2.5 Runge-Kutta Methods

Runge-Kutta methods are single-step, but multistage, time discretizations. The modified Euler version of a *second-order Runge-Kutta* (RK2) *method* can be written

$$\mathbf{u}^{n+1} = \mathbf{u}^n + \frac{1}{2}\Delta t[\mathbf{f}(\mathbf{u}^n, t^n) + \mathbf{f}(\mathbf{u}^n + \Delta t\mathbf{f}(\mathbf{u}^n, t^n), t^n + \Delta t)] . \tag{D.2.15}$$

A popular *third-order Runge-Kutta* (RK3) *method* is

$$\begin{aligned} \mathbf{k}_1 &= \mathbf{f}(\mathbf{u}^n, t_n) \\ \mathbf{k}_2 &= \mathbf{f}(\mathbf{u}^n + \tfrac{1}{2}\Delta t\ \mathbf{k}_1, t_n + \tfrac{1}{2}\Delta t) \\ \mathbf{k}_3 &= \mathbf{f}(\mathbf{u}^n + \tfrac{3}{4}\Delta t\ \mathbf{k}_2, t_n + \tfrac{3}{4}\Delta t) \\ \mathbf{u}^{n+1} &= \mathbf{u}^n + \tfrac{1}{9}\Delta t[2\mathbf{k}_1 + 3\mathbf{k}_2 + 4\mathbf{k}_3] . \end{aligned} \tag{D.2.16}$$

The classical *fourth-order Runge-Kutta* (RK4) *method* is

$$\begin{aligned}
\mathbf{k}_1 &= \mathbf{f}(\mathbf{u}^n, t_n) \\
\mathbf{k}_2 &= \mathbf{f}(\mathbf{u}^n + \tfrac{1}{2}\Delta t\, \mathbf{k}_1, t_n + \tfrac{1}{2}\Delta t) \\
\mathbf{k}_3 &= \mathbf{f}(\mathbf{u}^n + \tfrac{1}{2}\Delta t\, \mathbf{k}_2, t_n + \tfrac{1}{2}\Delta t) \\
\mathbf{k}_4 &= \mathbf{f}(\mathbf{u}^n + \Delta t\, \mathbf{k}_3, t_n + \Delta t) \\
\mathbf{u}^{n+1} &= \mathbf{u}^n + \tfrac{1}{6}\Delta t[\mathbf{k}_1 + 2\mathbf{k}_2 + 2\mathbf{k}_3 + \mathbf{k}_4] \; .
\end{aligned} \tag{D.2.17}$$

All Runge-Kutta methods of a given order have the same stability properties. The absolute stability regions are given in Fig. D.2 (right) and the stability boundaries along the axes are given in Table D.1. Note that the stability region expands as the order increases. Note also that RK2 methods are afflicted with the same weak instability as the AB2 scheme. When storage is not an issue, then the classical RK4 method is commonly used. Otherwise, the low-storage versions of third- and fourth-order methods, such as those described in Sect. D.4, have been preferred.

In the event that $\mathbf{f}$ contains no explicit dependence upon t, the following formulation, due to Jameson, Schmidt and Turkel (1981) applies:

$$\begin{aligned}
&Set \\
&\qquad \mathbf{u} = \mathbf{u}^n \\
&For\ k = s,\ 1,\ -1 \\
&\qquad \mathbf{u} \leftarrow \mathbf{u}^n + \frac{1}{k}\Delta t \mathbf{f}(\mathbf{u}) \\
&End\ For \\
&\qquad \mathbf{u}^{n+1} = \mathbf{u} \; .
\end{aligned} \tag{D.2.18}$$

It yields a Runge-Kutta method of order s (for linear problems) and requires at most three levels of storage.

D.3 Integrating Factors

For some applications of spectral methods the use of an *integrating-factor technique* is attractive. The Burgers equation (3.1.1) with periodic boundary conditions will serve here as a simple illustration of handling constant-coefficient linear terms via integrating factors. The semi-discrete Fourier Galerkin formulation of this is given by (3.3.3), which we write here as

$$\frac{\mathrm{d}\hat{u}_k}{\mathrm{d}t} + \hat{g}_k(\hat{\mathbf{u}}) + \nu k^2 \hat{u}_k = 0 \; , \qquad k = -\frac{N}{2}, \ldots, \frac{N}{2} - 1 \; , \tag{D.3.1}$$

where $\hat{g}_k(\hat{\mathbf{u}})$ is given by the right-hand side of (3.3.4). Equation (D.3.1) can be written

$$\frac{\mathrm{d}}{\mathrm{d}t}[e^{\nu k^2 t}\hat{u}_k] = -e^{\nu k^2 t}\hat{g}_k(\hat{\mathbf{u}}) \ .$$

The forward Euler approximation reduces to

$$\hat{u}_k^{n+1} = e^{-\nu k^2 \Delta t}[\hat{u}_k^n - \Delta t \hat{g}_k(\hat{\mathbf{u}}^n)] \ . \tag{D.3.2}$$

The treatment of the linear term is both unconditionally stable and exact. The accuracy and stability restrictions of the overall time-integration method arise solely from the nonlinear term.

The Fourier collocation method can be handled in a similar, but not equivalent manner:

$$\mathbf{u}^{n+1} = C^{-1}\Lambda C\mathbf{u}^n - \Delta t\mathbf{g}(\mathbf{u}^n) \ , \tag{D.3.3}$$

where $\mathbf{u}$ represents the vector of unknowns at the collocation points, C represents the discrete Fourier transform matrix (see (2.1.25) and (4.1.9)), $\mathbf{g}(\mathbf{u})$ represents the nonlinear advection term, and

$$\Lambda = \mathrm{diag}\left\{e^{-\nu k^2 \Delta t}\right\} \ . \tag{D.3.4}$$

This approach was used by Fornberg and Whitham (1978) on the Korteweg-de Vries equation

$$\frac{\partial u}{\partial t} + u\frac{\partial u}{\partial x} + \frac{\partial^3 u}{\partial x^3} = 0 \tag{D.3.5}$$

in their Fourier collocation-leap frog calculations. In this application, exact integration enables the stability limit to be increased from $\Delta t < (1/\pi^3)\Delta x^3$ to $\Delta t < (3/2\pi^2)\Delta x^3$. This is a fivefold increase. Note, however, that the $O(\Delta x^3)$ limit does not disappear entirely in favor of an $O(\Delta x)$ limit, as it would for a Fourier Galerkin method applied in conjunction with exact integration. Chan and Kerkhoven (1985) discuss alternative time discretizations of the Korteweg-de Vries equations. They show that, with the leap frog method for the advection term and the Crank-Nicolson method for the linear term, the stability limit is independent of Δx for any finite time interval.

The integrating-factor technique has found extensive use in Fourier Galerkin simulations of homogeneous turbulence (Rogallo (1977); see also CHQZ3, Sect. 3.3) and has also been used for the horizontal diffusion terms in calculations of parallel boundary layers (Spalart (1986); see also CHQZ3, Sect. 3.4.5). The integrating factors are especially useful in these Navier-Stokes applications because they do not suffer from the weak or nonexistent damping of the high-frequency components that arise in backward Euler or Crank-Nicolson discretizations of the viscous terms. Maday, Patera and Rønquist (1990) developed an integrating factor technique that is particularly useful in splitting methods. See CHQZ3, Sect. 3.2.3 for additional discussion.

D.4 Low-Storage Schemes

When high-order discretization schemes such as spectral methods are employed in space, the primary contributor to the error in the fully discrete approximation is usually the temporal discretization error unless the time discretization itself is at least third order or the time-step is very small. When computations are constrained by memory limitations, a premium is placed on minimizing storage demands. This has made special low-storage Runge-Kutta methods very attractive for large-scale problems. Several popular low-storage Runge-Kutta methods are available that permit third-order or fourth-order temporal accuracy to be obtained with only two levels of storage. Such economies are not available for multistep methods.

We shall note here some of the low-storage Runge-Kutta methods that have been widely used for large-scale spectral computations. The description shall be given for the ODE

$$\frac{\mathrm{d}\mathbf{u}}{\mathrm{d}t} = \mathbf{g}(\mathbf{u}, t) + \mathbf{l}(\mathbf{u}, t) \; . \tag{D.4.1}$$

where $\mathbf{g}(\mathbf{u}, t)$ is treated with a low-storage Runge-Kutta method and $\mathbf{l}(\mathbf{u}, t)$ is treated implicitly with the Crank-Nicolson method. Such mixed explicit/ implicit time discretizations are very common for incompressible Navier-Stokes computations, for which $\mathbf{g}(\mathbf{u}, t)$ represents (nonlinear) advection and $\mathbf{l}(\mathbf{u}, t)$ (linear) diffusion.

The general representation of a low-storage Runge-Kutta/Crank-Nicolson method requiring only 2 levels of storage (for $\mathbf{u}$ and $\mathbf{h}$) is

$$\begin{aligned}
&\mathbf{h} = \mathbf{0} \\
&\mathbf{u} = \mathbf{u}^n \\
&For\ k = 1\ to\ K \\
&\quad t^k = t^n + \alpha_k \Delta t \\
&\quad t^{k+1} = t^n + \alpha_{k+1} \Delta t \\
&\quad \mathbf{h} \leftarrow \mathbf{g}(\mathbf{u}, t^k) + \beta_k \mathbf{h} \\
&\quad \mu = \frac{1}{2} \Delta t (\alpha_{k+1} - \alpha_k) \\
&\quad \mathbf{v} - \mu \mathbf{l}(\mathbf{v}, t^{k+1}) = \mathbf{u} + \gamma_k \Delta t \mathbf{h} + \mu \mathbf{l}(\mathbf{u}, t^k) \\
&\quad \mathbf{u} \leftarrow \mathbf{v} \\
&End\ For \\
&\mathbf{u}^{n+1} = \mathbf{u}
\end{aligned} \tag{D.4.2}$$

(note that the penultimate instruction in the loop indicates that **v** is the solution of the implicit equation on the left-hand side).

Table D.2 lists the values of these parameters for one third-order scheme, due to Williamson (1980), and one fourth-order scheme from Carpenter and Kennedy (1994). The stability limits (on the imaginary axis) for these schemes are 1.73 for the third-order scheme and 3.34 for the fourth-order scheme. Both of these have been widely used for the time discretization in applications of spectral methods. Both references contain a family of low-storage methods. Another low-storage family popular in the spectral methods community originated with A. Wray (unpublished), and was extended by Spalart, Moser and Rogers (1993).

Table D.2. Coefficients of low-storage Runge-Kutta/Crank-Nicolson schemes

	Williamson 3rd-order	Carpenter-Kennedy 4th-order
α_1	0	0
α_2	1/3	0.1496590219993
α_3	3/4	0.3704009573644
α_4	1	0.6222557631345
α_5	–	0.9582821306748
α_6	–	1
β_1	0	0
β_2	-5/9	-0.4178904745
β_3	-153/128	-1.192151694643
β_4	–	-1.697784692471
β_5	–	-1.514183444257
γ_1	1/3	0.1496590219993
γ_2	15/16	0.3792103129999
γ_3	8/15	0.8229550293869
γ_4	–	0.6994504559488
γ_5	–	0.1530572479681